The Tensile Properties and Creep Performance of a Long-term Thermally Aged Plastic Bonded Explosive

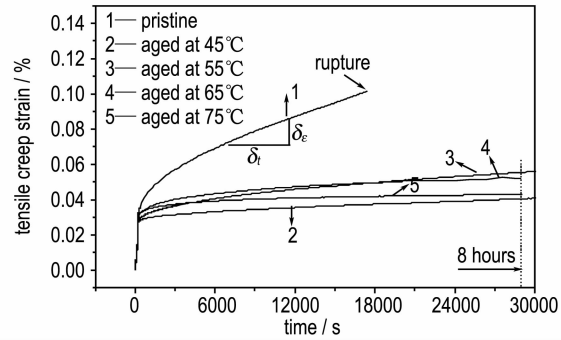

ZHOU Hong-ping, HE Qiang, LI Ming, PANG Hai-yan, WEI Xing-wen, WEN Mao-ping

Chinese Journal of Energetic Materials, 2016, 24(9): 826–831

Tensile creep curves of pristine (marked "1" in the plot) and 3 year stored specimens (2, 3, 4 and 5) at different temperature, all tests were performed under 2.88 MPa and 45 ℃.

Constitutive Behavior of RDX-based PBX with Loading-history and Loading-rate Effects

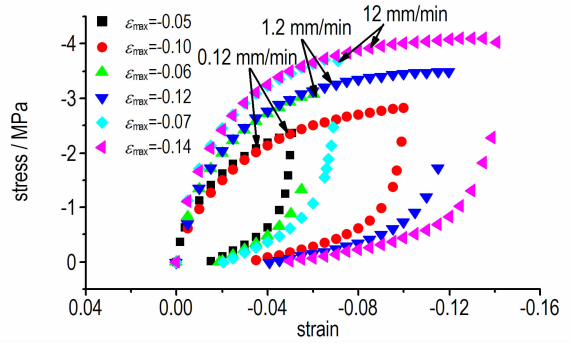

TANG Ming-feng, PANG Hai-yan, LAN Lin-gang, WEN Mao-ping, LI Ming

Chinese Journal of Energetic Materials, 2016, 24(9): 832–837

The cyclic loading and unloading stress-strain curves of cast PBX in the quasi-static strain rate range of 10^{-4}–10^{-2}/s were obtained by a material testing machine. The constitutive behavior of PBX was analyzed by Dorfmann and Ogden's model.

Energies of Combustion and Specific Heat Capacities of Diaminofurazan, Dinitrofurazan and Diaminoazofurazan

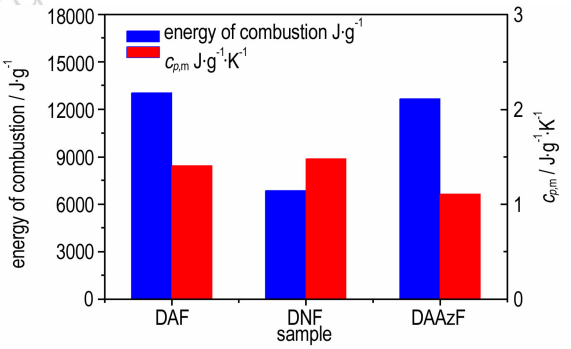

LI Yan-feng, ZHAI Lian-jie, XU Kang-zhen, SONG Ji-rong, ZHAO Feng-qi

Chinese Journal of Energetic Materials, 2016, 24(9): 838–841

Energies of combustion for the three furazan compounds tend to rise with the decrease of oxygen content in molecule. Amino group contributes to increase energy of combustion, but nitro group has the opposite effect. To specific heat capacity, the change rule for the three compounds is opposite to energy of combustion.

A Density Functional Theory Study on the Structures and Thermochemical Properties of Azo-bridged Azoles

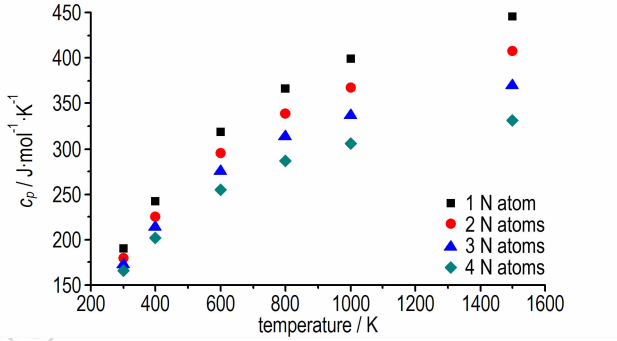

The structures and thermochemical properties of 15 kinds of azo-bridged azoles were studied by a density functional theory method to uncover the relationship between the structures and properties. B3LYP/6-311+G(d,p) level of theory was used to optimize the structures and calculate the thermochemical properties. The effect of the number and position of nitrogen atoms in azoles was discussed.

LAI Wei-peng, LIAN Peng, LIU Ying-zhe, YU Tao, LU Jian, WANG Bo-zhou, GE Zhong-xue

Chinese Journal of Energetic Materials,2016,24(9): 842–847

Thermal Behaviors of 1-Amino-2-nitroguanidine

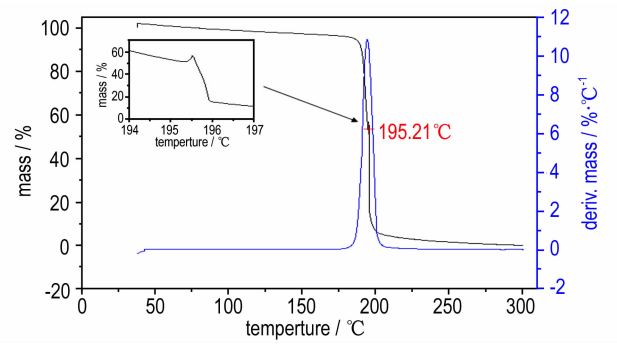

Thermal behaviors, specific heat capacity and adiabatic time-to-explosion of 1-amino-2-nitroguanidine(ANQ) were studied by DSC, micro-DSC and TG/DTG methods to further evaluate its thermal stability and investigate the potential application value as energetic material.

LI Yan-feng, WANG Meng-jie, XU Kang-zhen, SONG Ji-rong, ZHAO Feng-qi

Chinese Journal of Energetic Materials,2016,24(9): 848–852

Synthesis and Thermal Properties of 1,1′-Dioxide-5,5′-azotetrazole Dipotassium Salt

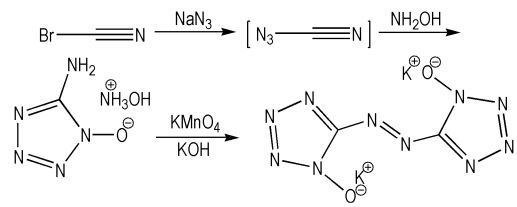

1,1′-Dioxide-5,5′-azotetrazole dipotassium salt was synthesized using cyanogen bromide, sodium azide and 50% solution of hydroxylamine as starting materials. The structure was characterized by IR, NMR and elemental analysis.

XIAO Xiao, YAO Er-gang, LIU Qing, SU Hai-peng, DING Ke-wei, GE Zhong-xue

Chinese Journal of Energetic Materials,2016,24(9): 853–856

An Insensitive Energetic Compound 5,7-Diamino-4,6-dinitrobenzotriazol-3-ium-1-oxide: Synthesis, Characterization and Performances

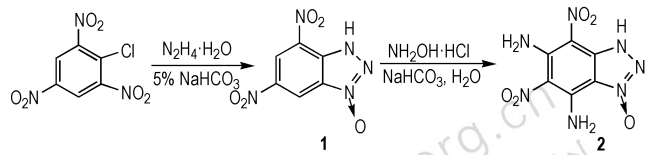

Using cheap and facile $NH_2OH \cdot HCl$ as a substitute for expensive THMI,5,7-diamino-4,6-dinitrobenzotriazol-3-ium-1-oxide was synthesized through cyclization and VNS reactions. The structure of the title compound and intermediate were characterized by ^1H NMR, ^{13}C NMR, FT-IR and elementary analysis. The detonation performances were calculated by Gaussian 09 and VLW equation.

HUO Huan, WANG Bo-zhou, ZHAI Lian-jie, BI Fu-qiang, DONG-Jun, LIAN Peng

Chinese Journal of Energetic Materials,2016,24(9): 857–861

Synthesis and Properties of 5-(3-Amino-1,2,5-oxadiazol-4-yl)tetrazol-1-ol and Its Ammonium and Hydroxylammonium Salts

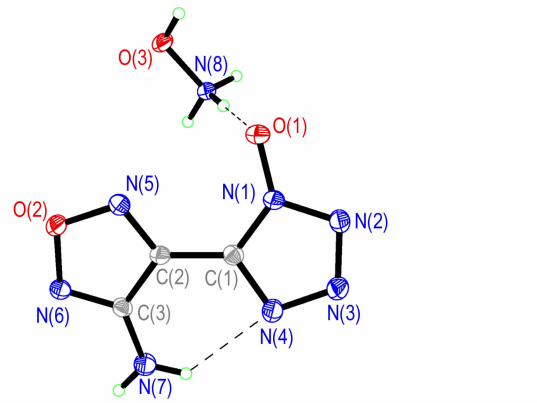

The synthesis and properties of 5-(3-amino-1,2,5-oxadiazol-4-yl)tetrazol-1-ol as well as its ammonium salt, and hydroxylammonium salt are described. X-ray single-crystal diffraction analysis indicates that the intramolecular and intermolecular hydrogen bonds of these compounds play a pivotal role on their molecular density, and thermal stability.

ZHAI Lian-jie, FAN Xue-zhong, WANG Bo-zhou, HUO Huan, LI Ya-nan, BI Fu-qiang, ZHANG Jun-lin

Chinese Journal of Energetic Materials,2016,24(9): 862–867

Coatings of Activated Metal Hydride and Application in the Fuel-rich Propellant

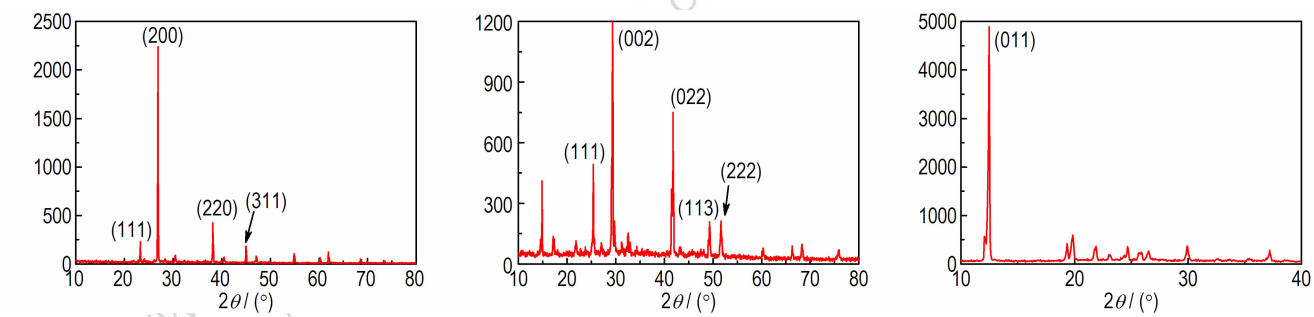

KBH_4 and $NaBH_4$ were coated by paraffin via solvent-nonsolvent method and $LiAlH_4$ was coated by naphthalene via recrystallization. The surface coating situation of the samples was studied by SEM, FTIR and XRD and the combustion properties of the propellants added into coated sample were tested by an infrared thermometer.

LIU Ting, CHEN Xin, HAN Ai-jun, YE Ming-quan, SHI Qing-yi, PAN Gong-pei

Chinese Journal of Energetic Materials,2016,24(9): 868–873

Crystal Structure and Thermal Behavior of Potassium Dinitromethane

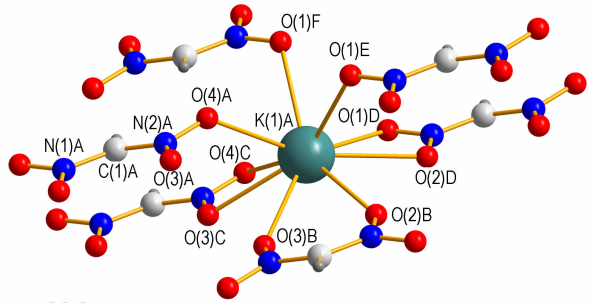

SUN Qian, WANG Xiao-hui, XU Kang-zhen, LI Yan-feng, SONG Ji-rong, ZHAO Feng-qi

***Chinese Journal of Energetic Materials*, 2016, 24(9): 874–879**

$\{K[CH(NO_2)_2]\}_n$ was obtained and characterized. $\{K[CH(NO_2)_2]\}_n$ crystallizes in triclinic system with space group *P*-1 containing two molecules per unit cell.

Investigation of the Phase Transitions of FOX-7 by Temperature-dependent FTIR Spectroscopy

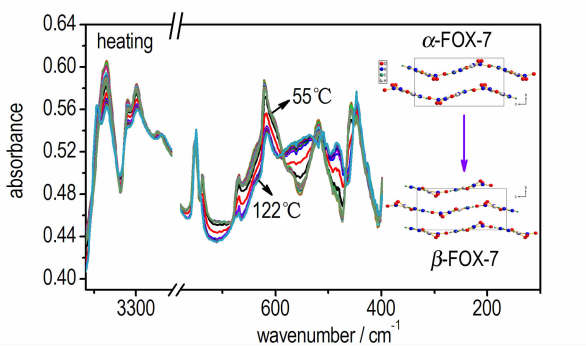

ZHANG Hong-li, LIU Yu, ZHANG Hao-bin, LI Shi-chun, ZHU Chun-hua, XU Jin-jiang, YANG Shi-yuan, LI Jin-shan

***Chinese Journal of Energetic Materials*, 2016, 24(9): 880–885**

Two kinds of phase transitions ($\alpha \rightarrow \beta$ and $\beta \rightarrow \gamma$) of 1,1-diamino-2,2-dinitroethylene (FOX-7) have been investigated by temperature-dependent Fourier transform infrared (FTIR) spectroscopy, and the effects of intermolecular H-bonding interactions and molecular structure in the phase transitions of FOX-7 were discussed.

Determination and Correlation of Solubility in Binary System Ethanol-Water of 3,4-Bis(3-nitrofurazan-4-yl)furoxan

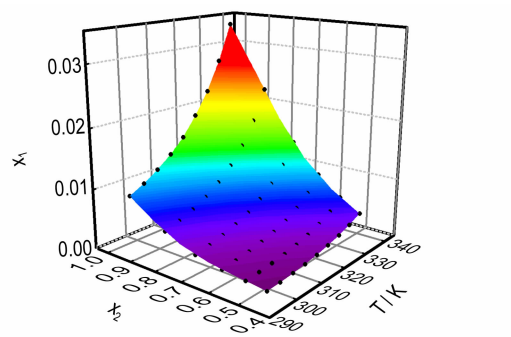

LAN Guan-chao, WANG Jian-long, CAO Duan-lin, CHEN Li-zhen, HOU Huan, LI Jing

***Chinese Journal of Energetic Materials*, 2016, 24(9): 886–891**

The solubility of DNTF from 298.15 K to 338.15 K was determined by using a laser monitoring system under atmospheric pressure. The relationship between the temperature and the ethanol ratio was obtained.

Fabrication and Flyer Driving Capability Characterisation of an Integrated Exploding Foil Initiator

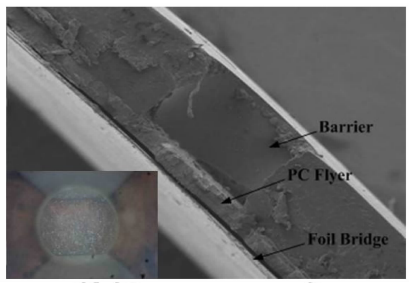

Photolithography and CVD techniquesare employed to fabricate an integrated EFI with Parylene C flyer and Su8-2150 barrier. The Photonic Doppler Velocimetry is also been adopted for the parameter research of integrated EFI's performance, the result seems that the velocity characteristic profile of the integrated EFI is similar to the one fabricated with polyimide flyer and steel barrier. In addition the HNS-Ⅳ is successfully been detonated by the integrated EFI.

FANG Kuang, CHEN Qing-chou, FU Qiu-bo, WANG Yao
Chinese Journal of Energetic Materials,2016,24(9): 892–897

Numerical Study on Deformation and Ignition Process of Impacting Granular HMX Explosive in Drop Hammer Test

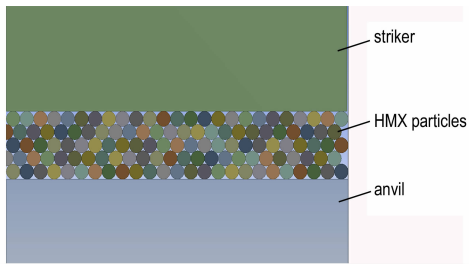

Two-dimensional numerical simulation of the impact process for drop hammer on granular HMX was carried out by using ANSYS/AUTODYN software. The temperature rise generated in particles was estimated via the principle converted from plastic work to heat energy based on the calculated values of stress and plastic work.

YIN Lu, LIU Zhi-yue, WANG Li-qiong
Chinese Journal of Energetic Materials,2016,24(9): 898–904

Shock Initiation Characteristics of Explosives at Near-ambient Temperatures

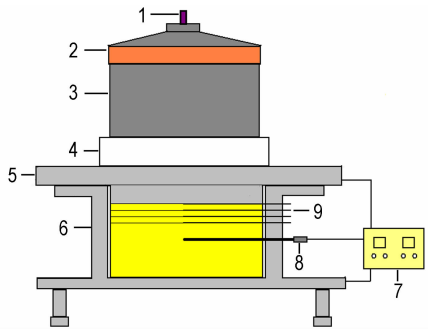

An experimental device with local heating and cooling to explosive was designed and established to study the influence extent and law of near-ambient temperature changes on shock initiation characteristics of explosives, combined with Lagrangian analysis method, the growth process of shock initiation pressure at the near room temperature from 5 ℃ to 75 ℃ for two explosives (PBX-1: a HMX/TATB composite explosive; PBX-2: a TATB based IHE) was studied. Based on the experimental results, numerical simulation of the shock initiation process for two kinds of explosives was performed by the model of ignition growth.

TAN Kai-yuan, WEN Shang-gang, HAN Yong
Chinese Journal of Energetic Materials,2016,24(9): 905–910

Short Duration Pulse Shock Initiation Characteristics of Ultrafine LLM-105

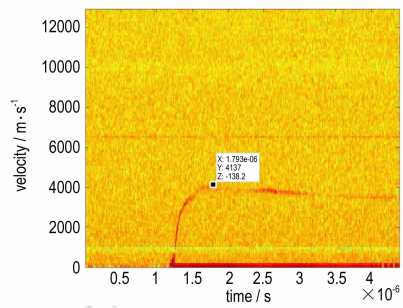

The initiation system of high velocity flyer has been obtained by PDV. The initiation threshold testing is complemented of ultrafine LLM-105. The initiation threshold testing has been implemented by small dimension flyer of ultrafine LLM-105 explosive. The 50% firing current is 2.14 kA which is equal to HNS-Ⅳ.

FU Qiu-bo, LI Min, GUO Fei, WANG Meng, WANG Yao
Chinese Journal of Energetic Materials,2016,24(9): 911–914

The Initiation Parameter of Detonation Wave Aiming Warhead

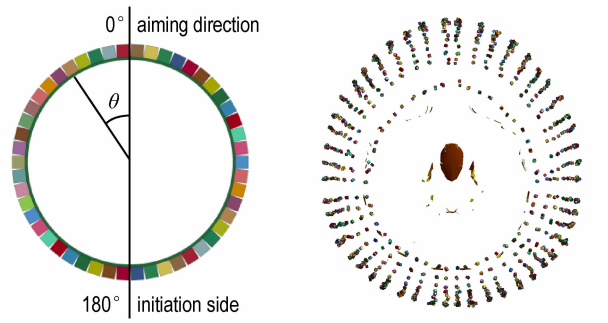

The verified numerical model was used to thoroughly research the influences of initiation styles and parameters on the warhead lethality. The velocity enhancements in the aiming direction were compared and the optimal initiation types were selected. The rules underlying the enhancement results were also investigated.

LI Yuan, LI Yan-hua, LIU Chen, WEN Yu-quan
Chinese Journal of Energetic Materials,2016,24(9): 915–921

3,4-Bis(3-fluorodinitromethylfurazan-4-oxy)furazan: A New Thermally Stable Plasticizer with High Energy Density

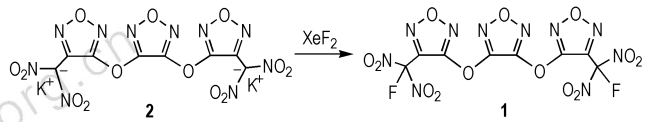

An excellent energetic plasticizer 3,4-bis(3-fluorodinitromethylfurazan-4-oxy)furazan was self-designed and synthesized, and its main energetic properties were investigated.

ZHAI Lian-jie, FAN Xue-zhong, WANG Bo-zhou, LIAN Peng, ZHOU Cheng, HUO Huan, LI Ya-nan, BI Fu-qiang
Chinese Journal of Energetic Materials,2016,24(9): 922–924

Synthesis and Characterization of a Novel Energetic Inner-salt 5,5′-Bis(3-diazo-1,2,4-triazole)

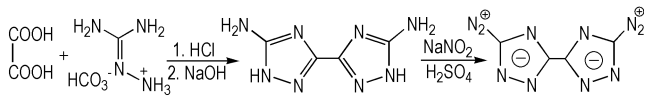

A novel energetic inner-salt 5,5′-bis(3-diazo-1,2,4-triazole) was firstly designed and synthesized by cyclodehydration, diazotization reactions with a total yield of 53.0%, and its structure was confirmed. Theoretical calculations at 3LYP/6-311G+(d,p) level were performed, and the results show that the density is 1.73 g·cm^{-3}, the D_v is 7780 m·s^{-1} and D_p is 26.72 GPa.

LUO Yi-fen, ZHAI Lian-jie, BI Fu-qiang, ZHOU Cheng, WANG Bo-zhou
Chinese Journal of Energetic Materials,2016,24(9): 925–926